Performance assessments of absorbing conditions for the reverse time-harmonic migration

Hélène Barucq, Morgane Bergot, Juliette Chabassier, Julien Diaz

1st Pan-American Congress on Computational Mechanics - PANACM 2015
XI Argentine Congress on Computational Mechanics - MECOM 2015
S. Idelsohn, V. Sonzogni, A. Coutinho, M. Cruchaga, A. Lew & M. Cerrolaza (Eds)

PERFORMANCE ASSESSMENT OF ABSORBING CONDITIONS FOR THE REVERSE TIME-HARMONIC MIGRATION

Hélène Barucq[1], Morgane Bergot[2], Juliette Chabassier[1] and Julien Diaz[1]

[1] Inria Team-Project Magique-3D, University of Pau, France
helene.barucq@inria.fr, juliette.chabassier@inria.fr

[2]Institut Camille Jordan, University Claude Bernard Lyon 1, France
bergot@math.univ-lyon1.fr

Key words: Wave Propagation, Numerical Simulation, Absorbing Boundary Condition, Reverse Time Migration

Abstract. We propose an imaging technique based on the solution of harmonic wave equations. Its principle is inspired by the Reverse Time Migration which is widely used for seismic imaging. The numerical method involves Radiation Boundary Conditions and we assess the impact of these conditions on the capability of the imaging method to recover an obstacle hidden inside a fluid.

1 INTRODUCTION

Waves are widely used for providing images of the subsurface. By making use of their reflection capabilities, it is possible to create a map identifying each change of medium. This map deserves a particular attention because it contains relevant information on the material characteristics of the propagation domain without requiring any extraction process. Reverse Time Migration (RTM) is an imaging technique based on the solution of time-dependent wave equations set inside bounded regions given as the domain to be explored. RTM provides a way for putting time information recorded by some receivers back to the piece of subsurface of interest. RTM is well-known to be a robust seismic imaging technique but it is computationally intensive. It is indeed based on the solution of a large number of wave equations that distinguish themselves by the source term and the construction of the image requires a pre-processing step which often reaches the limitations of the memory. There is thus a need in optimizing the computational costs of RTM. Several tries have been achieved by developing new numerical schemes for High-Performance Computing (HPC) of wave equations [4, 6]. It turns out that numerical costs can be reduced but this improvement is limited by the validity domain of the discretization. Reducing numerical costs actually gives advantage to explicit time-schemes

which work under stability conditions. Obeying the stability condition then freezes the reduction of computational costs. Moreover, the construction of the image is based upon a discrete imaging operator defined on a cartesian grid which needs to be fine to capture heterogenities correctly. As a consequence, RTM is not easy to put in action when targeting realistic problems because it generates a huge computational burden shared between computational time and memory storage. We then propose to assess the performance of RTM in the harmonic domain by suiting the RTM algorithm to harmonic waves for providing images more quickly. Our approach is different from what is done for Full Waveform Inversion since we do not minimize a cost function. By this way, we may avoid issues of local minima while taking advantage of the robustness of harmonic equations in the sense that we do not have to perform any time discretization.
This paper provides preliminary results for motivating our solution methodology. We address a simpler problem which consists in recovering the shape of an obstacle. The computational domain is limited by an artificial boundary and the numerical waves are then obtained by solving harmonic wave equations coupled with specific boundary conditions on the artificial boundaries which are generally referred as Absorbing Boundary Conditions (ABC) [12] in the time-domain or Radiation Boundary Conditions (RBC) [9] in the harmonic domain. It is well-known that the accuracy of the solution to Helmholtz equation depends on the RBC that is employed. This is why, in addition to the validation of a harmonic-wave seismic imaging technique, we investigate how the RBC can impact on the quality of the image.

2 RADIATION BOUNDARY CONDITIONS

In this section, we introduce the boundary conditions that we use for solving the Helmholtz equation. Their derivation is explained in detail in an internal report [5] dealing with high-order artificial boundary conditions both for the harmonic and time-dependent wave equation. We recall that the Helmholtz equation reads as:

$$\frac{\omega^2}{c^2}u + \Delta u = 0, \tag{1}$$

where ω denotes the pulsation and c is the propagation velocity. The equation is set in a two-dimensional bounded domain Ω with an external boundary Σ representing the artificial boundary. Let $\kappa(s)$ be the curvature of the boundary Σ, s denoting the curvilinear coordinate. We then consider the first order familiy of RBCs which are given by:

$$k = \frac{\omega}{c}, \quad (\partial_{\mathbf{n}}u + ik\,u) + \left(\gamma + \frac{\kappa}{4}\right)\,u + \left(\gamma - \frac{\kappa}{4}\right)\,\frac{\partial_{\mathbf{n}}u}{ik} = 0, \tag{2}$$

where γ denotes a parameter and $\mathbf{n}$ stands for the normal vector on Σ outwardly directed to Ω. It has be proven in [7] that if γ is larger than $\kappa(s)/4$, then the boundary value

problem of Helmholtz equation coupled with this RBC is well-posed. When γ is equal to $\kappa(s)/4$, we get the most widely used RBC for the Helmholtz problem:

$$\partial_r u + ik\, u + \frac{\kappa}{2}\, u = 0. \tag{3}$$

The condition is often referred to as "curvature-RBC" or "C-RBC" ([14, 13, 9]). The conditions (2) have been derived by approximating a non-reflecting boundary condition under the assumption that the waves impinge the boundary with an incidence angle close to the normal one. It is interesting to note that RBCs can also be constructed by assuming the frequency ω is high. In that case, the lowest-order approximation gives rise to:

$$k = \frac{\omega}{c}, \qquad \partial_r u + ik\, u + \left(\gamma + \frac{\kappa}{4}\right) u = 0. \tag{4}$$

Then it is worth to note that the specific value $\gamma(s) = \dfrac{\kappa(s)}{4}$ also leads to the "C-RBC" previously obtained in [14, 13, 9]. By performing the next order of approximation, we then have:

$$k = \frac{\omega}{c}, \quad \left[1 + \frac{\gamma - \dfrac{\kappa}{4}}{ik}\right] \partial_{\mathbf{n}} u + \left[ik + \gamma + \frac{\kappa}{4}\right] u - \frac{1}{2\,ik}\Delta_\Sigma u = 0. \tag{5}$$

When $\gamma(s) = \dfrac{\kappa(s)}{4}$, we get a well-known second-order RBC:

$$\partial_n u + iku + \frac{\kappa(s)}{2} u - \frac{1}{2ik}\Delta_\Sigma u = 0. \tag{6}$$

3 NUMERICAL IMAGING BASED ON HARMONIC WAVE SOLUTIONS

The Reverse Time Migration [11] is based on the cross-correlation of waves. The numerical waves are divided into two groups: waves generated by sources and numerical waves corresponding to the back-propagation of reflected waves. The cross-correlation of these two groups gives then the picture of reflectors, that is each point of the propagation domain where reflections occur. We follow the same algorithm but by solving harmonic wave equations. We then have a first group of numerical waves generated by source points x_j, $j = 1, ..., N$, which are dispatched regularly around a penetrable obstacle inside the computational domain (see Fig. 1). The waves are reflected by the boundary of the obstacle to be detected and the reflected waves are recorded by sensors. Then the

recordings provide a set of complex data which are conjugated and used as sources in the Helmholtz problem. By this way, we solve the conjugate set of equations which amounts to back-propagate the reflected waves. We then end up with solving two Helmholtz problems with multiple right-hand sides given as the different sources. The procedure to follow is then:

Propagation of sources: solve

$$\begin{cases} \dfrac{\omega^2}{c^2} u_{S_j} + \Delta u_{S_j} = S_j, j = 1, ..., N, \\ \text{RBC on } \Sigma. \end{cases} \tag{7}$$

where S_j, $j = 1, ..., N$ denotes a point source at a given point x_j: $S_j = \delta_{x_j}$. For each j, record $u_{S_J}(x_i), i = 1, ..., N$.

Back-propagation of reflected waves: solve

$$\begin{cases} \dfrac{\omega^2}{c^2} u_{R_j} + \Delta u_{R_j} = \displaystyle\sum_{i=1}^{N} \bar{u}_{S_j}(x_i)\delta_{x_i}, j = 1, ..., N, \\ \text{RBC on } \Sigma. \end{cases} \tag{8}$$

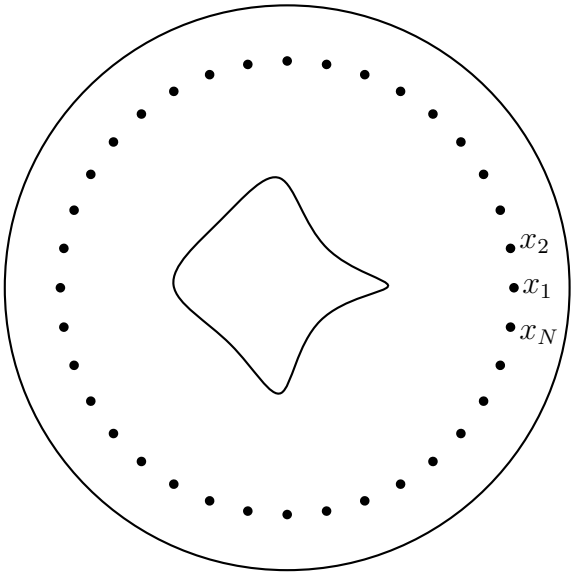

Figure 1: Position of the sources and of the obstacle

When real data are not available, the first experiment must be performed twice to provide a set of data. In that case, we construct the set of data by using another numerical method. By this way, we avoid inverse crime.

Once the two problems have been solved, we need to construct the image by applying an imaging condition. Herein, we propose the imaging operator I defined at each point x of the numerical grid by:

$$I(x) = \sum_{j=1}^{N} \Re e(u_{S_j}(x) * u_{R_j}(x)).$$

4 NUMERICAL RESULTS

The numerical experiments are performed by using an Interior Penalty Discontinuous Galerkin approximation [1] that is implemented in the code Hou10ni, using curved elements to discretize the external boundary and the obstacle. We refer to [8] for more details on the implementation of Hou10ni. The computational domain is a circle of radius 2km, the obstacle has the shape presented in Fig 1. Inside the obstacle, we set $c = 2200$ m/s and outside the obstacle we set $c = 1500$ m/s. We use 100 sources placed on a circle of radius 1.9 km (very close from the boundary) and we set the frequency $\omega = 50$ Hz. We have used finite elements of degree 4. The global linear system is solved with Mumps, using the multi-right hand side feature. This feature is another advantage of harmonic RTM compared with time-dependent RTM, which requires to solve one wave equation for each source.

For the time being, we have consider the family of RBCs (4) for various values of γ. It turns out that all the images have the same quality and that we are always able to identify the obstacle. That is why we set only a picture (see Fig.4) which illustrates the capability of the numerical method to reconstruct the shape of the obstacle.
We are thus able to identify the obstacle by applying the extension of RTM in the harmonic regime. We have considered various RBCs and they all provide the same solution. More numerical experiments are needed to conclude because we have considered a simple case where the artificial boundary is a circle. In that particular case, it has been demonstrated (see for instance [7]) that all the conditions (4) are equivalent. High-order conditions should thus be considered with different shapes of artificial boundary.

5 Concluding remark: about injecting grazing wave modeling

It has been illustrated in [7] that the lack of performance of classical RBCs may come from the fact that the grazing waves are not controlled by the usual RBCs. Following page 140 of [7], it is possible to enforce the control of grazing waves by modifying classical RBCs. For instance, the modified C-RBC reads as:

$$\left[1 + \frac{c - \kappa/2}{ik}\right] \partial_{\mathbf{n}} u + \left[ik + c + \frac{\kappa\, c}{2ik}\right] u - \frac{1}{ik}\Delta_{\Sigma} u = 0. \tag{9}$$

For example, let us consider the case where the obstacle is a sound-soft elongated ellipse. We solve the first problem with one source and we apply the modified C-RBC on the artificial boundary Σ. Its shape is in keeping with the shape of the obstacle. The parameters

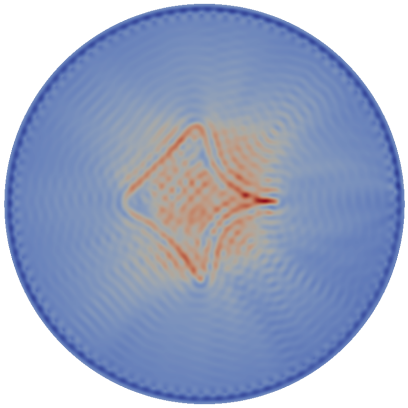

Figure 2: RTM Image

Freq	R_{rbc}	r_{rbc}	C-RBC	C-RBC + Grazing	C-RBC Δ	C-RBC Δ + Grazing
1	5.05	0.505	45.16	23.92	16.98	21.01
2	5.05	0.505	39.41	11.56	14.81	10.55
4	5.05	0.505	38.79	6.91	15.38	5.02

Table 1: Ellipse performances

of the obstacle are 0.5 for the small axis and 5 for the large axis. The reference solution is computed by solving the Helmholtz equation coupled with a non-reflecting boundary condition [10] set on a boundary which must be put far enough from the obstacle. Basically, it is necessary to have several wavelengths between the obstacle and the artificial boundary. However, the numerical solution obtained with the modified RBC is computed by using an artificial boundary which is set very close to the obstacle (see figure 3). The real part of the reference solution u_{ref} is displayed for a frequency equal to 1 (see figure 3). The table 5 shows that adding the modeling of grazing waves improves the relative L2-norm error err defined by

$$err = \sqrt{\frac{\int_\Omega |u - u_{ref}|^2}{\int_\Omega |u_{ref}|^2}}.$$

This is particularly clear when the frequency increases.

We thus observe that there is an advantage in including grazing waves inside the external boundary condition. In the context of seismic imaging involving harmonic waves, we now aim at investigating if by using this kind of condition, it might be possible to put the artifical boundary closer to the sources. This could contribute to reduce the computational costs. According to a previous work on On-Surface-Radiation Conditions [3], we believe that modified RBCs including grazing wave modeling might help. Anyway, modified RBCs should improve the quality of the image since it has been shown in [7] that the

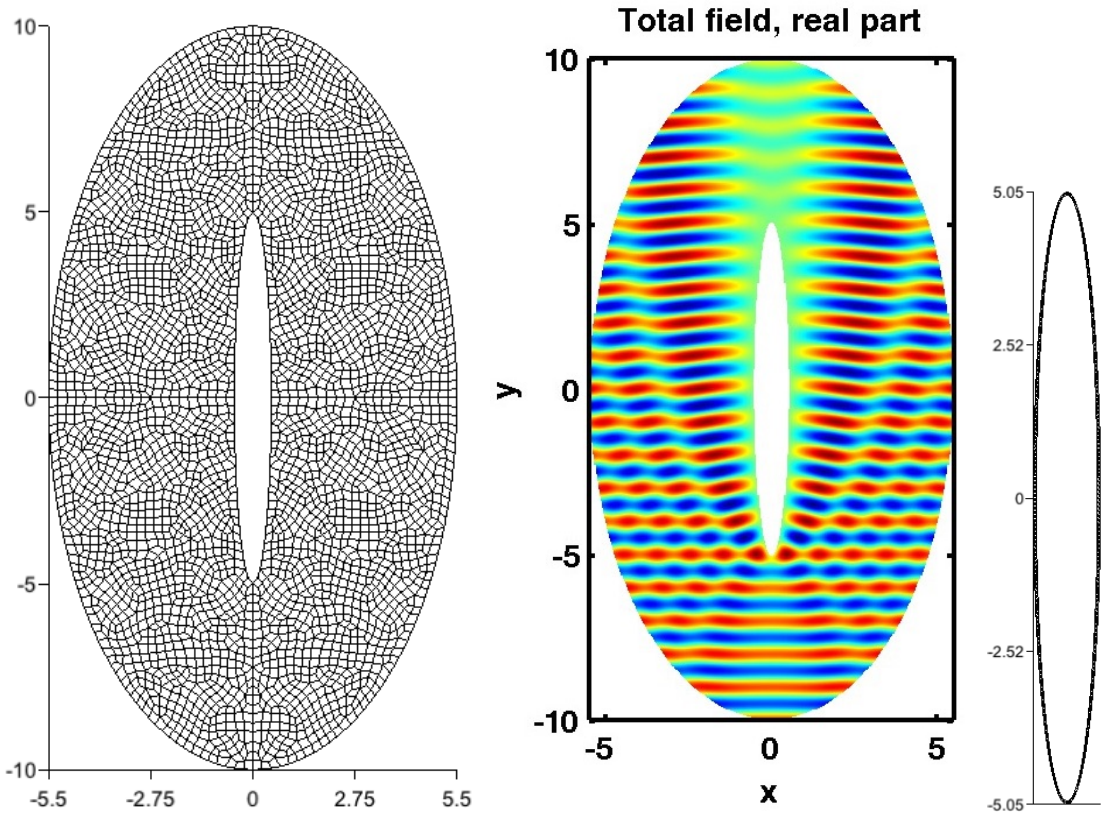

Figure 3: Ellipse

solution of the Helmholtz equation is really more accurate. However, these conditions involve higher order differential operators which means that their numerical handling will increase the computational burden. This point deserves a particular attention because this could be an inconvenient when considering three-dimensional problems.

REFERENCES

[1] M. Ainsworth, P. Monk and W. Muniz. Dispersive and Dissipative Properties of Discontinuous Galerkin Finite Element Methods for the second-Order Wave Equation *Journal of Scientific Computing*, vol 27 (1-3), pp 5-40, 2006.

[2] X. Antoine, H. Barucq, and A. Bendali. Bayliss-Turkel like radiation conditions on surfaces of arbitrary shape *J. Math. Anal. Appl.*, vol 229, pp 184-211, 1999.

[3] X. Antoine, M. Darbas, and Y. Y. Lu, An improved surface radiation condition for high-frequency acoustic scattering problems, *Computer Methods in Applied Mechanics and Engineering*, vol. 195(33), pp 4060-4074, 2006.

[4] C. Baldassari , H. Barucq, H. Calandra , and J. Diaz Numerical performances of a hybrid local-time stepping strategy applied to the reverse time migration. *Geophysical Prospecting*, 59 (5), 907-919 (2011).

[5] H. Barucq, M. Bergot, J. Chabassier, and E. Estecahandy. Derivation of high order absorbing boundary conditions for the Helmholtz equation in 2D. *Inria Research Report RR-8632*, (2014). http://hal.inria.fr/hal-01085180.

[6] H. Barucq, H. Calandra, J. Diaz, and F. Ventimiglia High-order time discretization of the wave equation by Nabla-p scheme *ESAIM: Proceedings*, 45, 67 74 (2014).

[7] H. Barucq, J. Diaz and V. Duprat. Long-Time Stability Analysis of Acoustic Absorbing Boundary Conditions for Regular-Shaped Surfaces. *Mathematical Models and Methods in Applied Sciences,* vol 23(11), pp 2129–2154, 2013.

[8] H. Barucq, R. Djellouli, and E. Estecahandy, Efficient DG-like formulation equipped with curved boundary edges for solving elasto-acoustic scattering problems. *International Journal for Numerical Methods in Engineering*, vol. 98 (10), pp. 747-780, 2014.

[9] A. Bayliss, M. Gunzburger, and E. Turkel. Boundary Conditions for the Numerical Solution of Elliptic Equations in Exterior Regions. *SIAM Journal on Applied Mathematics*, 42, 2, 430–451 (1982).

[10] M. Duruflé; Intégration numérique et éléments finis d'ordre élevé appliqués aux équations de Maxwell en régime harmonique. *PhD thesis of Dauphine University.* Paris, pp 253–262, 2006.

[11] J. Claerbout. Toward a unified theory of reflector mapping. *Geophysics*, vol. 36,1991

[12] B. Engquist and A. Majda. Absorbing Boundary Conditions for the Numerical Simulation of Waves. *Math. Of Comp.* 31, n139, 629-651 (1977).

[13] B. Hanouzet and M. Sesquès. Absorbing boundary conditions for Maxwells equations, in "Non-Linear Hyperbolic Problems: Theoretical, Applied and Computational Aspects". *A. Donato and F. Olivieri, Eds. Notes Numer. Fluid Dynamics*, vol 43, pp 315–322, 1992.

[14] B. Stupfel. Absorbing boundary conditions on arbitrary boundaries for the scalar and vector wave equations. *IEEE Trans. Antennas and Propagation*, vol 42(6), pp 773–780, 1994.